

## Combining deep learning and X-ray imaging technology to assess tomato seed quality

Herika Paula Pessoa<sup>1</sup>, Mariane Gonçalves Ferreira Copati<sup>\*1</sup>, Alcinei Místico Azevedo<sup>2</sup>, Françoise Dalprá Dariva<sup>1</sup>, Gabriella Queiroz de Almeida<sup>1</sup>, Carlos Nick Gomes<sup>1</sup>

<sup>1</sup>Universidade Federal de Viçosa – Depto de Agronomia, Av. P.H. Rolfs s/n – 36570-900 – Viçosa, MG – Brasil.

<sup>2</sup>Universidade Federal de Minas Gerais/Instituto de Ciências Agrárias, Av. Universitária, 1000 – 39404-547 – Montes Claros, MG – Brasil.

\*Corresponding author <mariane.goncalves@ufv.br>

Edited by: Sergio Tonetto de Freitas

Received August 01, 2022

Accepted March 13, 2023

**ABSTRACT:** Traditional germination tests which assess seed quality are costly and time-consuming, mainly when performed on a large scale. In this study, we assessed the efficiency of X-ray imaging analyses in predicting the physiological quality of tomato seeds. A convolutional neural network (CNN) called mask region convolutional neural network (MaskRCNN) was also tested for its precision in adequately classifying tomato seeds into four seed quality categories. For this purpose, X-ray images were taken of seeds of 49 tomato genotypes (46 *Solanum pennellii* introgression lines) from two different growing seasons. Four replicates of 25 seeds for each genotype were analyzed. These seeds were further assessed for germination and seedling vigor-related traits in two independent trials. Correlation analysis revealed significant linear association between germination and image-based variables. Most genotypes differed in terms of germination and seed development performance considering the two independent trials, except LA 4046, LA 4043, and LA4047, which showed similar behavior. Our findings point out that seeds with low opacity and percentage of damaged seed tissue and high values for living tissue opacity have greater physiological quality. In short, our work confirms the reliability of X-ray imaging and deep learning methodologies in predicting the physiological quality of tomato seeds.

**Keywords:** *Solanum lycopersicum*, computer vision, high throughput, germination

## Introduction

Seed quality is mainly assessed through germination and vigor tests. These manual methods of evaluation are time-consuming and subjective (Wu et al., 2019). Furthermore, they lead to seed destruction and are very lagging when working with many genotypes. Developing quick methods to evaluate seed quality traits on a large scale and with greater precision is therefore relevant.

Internal morphology and anatomical characteristics of seeds are correlated with seed quality. X-ray imaging is based on X-ray attenuation differences in different tissues, which means that it can reveal the internal morphology of seeds. X-ray images are emerging as a promising technique for inferring seed quality in several crop species (Noronha et al., 2018; Pinto et al., 2018; Vasconcelos et al., 2018; Medeiros et al., 2020b). Its advantages are mainly related to the possibility of evaluating many samples, ease of execution, low cost, and non-destruction of seeds (Kotwaliwale et al., 2014).

An extensive amount of data in the radiographic images must be analyzed to assess seed quality using X-ray imaging. Deep learning approaches such as convolutional neural networks (CNNs) are developed to learn features from data that come in the form of multiple arrays, such as video, text, sound, and images, including X-ray images (LeCun et al., 2015; Rippner et al., 2022; Sahin, 2023). The CNN models have succeeded in numerous practical applications, such as pattern and speech recognition and image classification (Altuntaş et al., 2019; Tajbakhsh et

al., 2016; Yu et al., 2018). As regards their use in agriculture, CNNs have proved to be efficient in performing image analysis in several different crops such as chrysanthemum (Wu et al., 2019), wheat (Jin et al., 2018), and oilseed rape (*Brassica napus* L.) (Yu et al., 2018). As for seed traits, recent studies have mentioned the use of CNN to extract information about seed images (Jin et al., 2018; Yu et al., 2018; Przybyło and Jabłoński, 2019; Wu et al., 2019; Nie et al., 2019; Pang et al., 2020).

In this work, we combined the computer vision of X-ray images and CNN to assess tomato seed quality from two consecutive growing seasons using the *Solanum pennellii* Corr. introgression line population as a crop model. Since the assessment of seed viability is currently performed manually, our approach is novel and promising. It could be the key to introducing machine vision systems in the seed technology industry.

## Materials and Methods

### Plant material

In this study, forty-six *S. pennellii* introgression lines (ILs) from the collection developed by Eshed and Zamir (1995), their genitors' cultivar M82 and the *S. pennellii* accession LA716, as well as the commercial tomato cultivar Santa Clara were evaluated. Seeds were multiplied over two different growing seasons in the Research and Extension Farm Unit Horta Velha at Universidade Federal de Viçosa, Viçosa, MG, Brazil (20°45'14" S, 42°52'53" W, 648.74 m altitude).

## Physiological analysis

A germination test followed by seedlings' evaluation was performed *in vitro* at the Seed Laboratory from the Agronomy Department of the Universidade Federal de Viçosa.

For the germination test, four repetitions of 25 seeds of each genotype and growing season were placed in disinfested plastic boxes containing two layers of germitest® paper moistened with distilled water (1:2.5, g mL). The boxes were then incubated in a germinator at a constant temperature of 25 °C and were visually examined daily for 14 days to register the number of germinated seeds. On the 14<sup>th</sup> day, seedling shoot and root length were measured manually using a digital pachymeter (Louisware® Stainless Steel Caliper 150 mm/0-6 inch).

The data from the daily counting of germinated seeds and seedling shoot and root length measurements were processed using the R software and the SeedCalc packages (Silva et al., 2019). The following variables were extracted: coefficient of variation of germination (CVG), coefficient of variation of germination time (CVT), final germination percentage (FGP), germination index (GI), growth index (Growth), mean root length (MRL), mean shoot length (MSL), uniformity index (Unif), vigor index (Vigor).

## X-ray imaging acquisition

Four repetitions of 25 seeds were fixed on adhesive paper for each genotype and growing season. This step allowed for the individual identification of each

seed so each seed could be individually analyzed in the following analysis.

The X-ray images were generated using the Faxitron MX-20 model (Faxitron X-ray Corp) device. The equipment was adjusted to a voltage of 23 kV. Image contrast had been calibrated to 16383 (width) × 3124 (center) as described by Medeiros et al. (2020a). The seeds were exposed to radiation for 10 s at a focal length of 41.6 cm. The images were saved in Tagged Image File Format (TIFF) files for further analysis (Figure 2A-D).

## Feature extraction

All data analyses (Figure 1) were performed using the R software. To compress the images, we used the image read and image scale functions from the magick package to allow for a quick computational analysis. Images were compressed to 400 pixels in width and 440 pixels in height. Soon after compression, images were processed by the *readImage* function from the *EBImage* package, which converts grayscale images into an array with values ranging from zero to one.

X-ray images were cropped into several single-seeded images with the help of the computed features moment from the *EBImage* package (Figure 2A-D). After this, the coordinates of each pixel on each seed were rotated to establish a longitudinal axis by principal components using the *princomp* function from the *stats* package. This longitudinal axis was further segmented into three equidistant portions. Pixels' coordinates belonging to each one of these portions were used to estimate: the percentage of

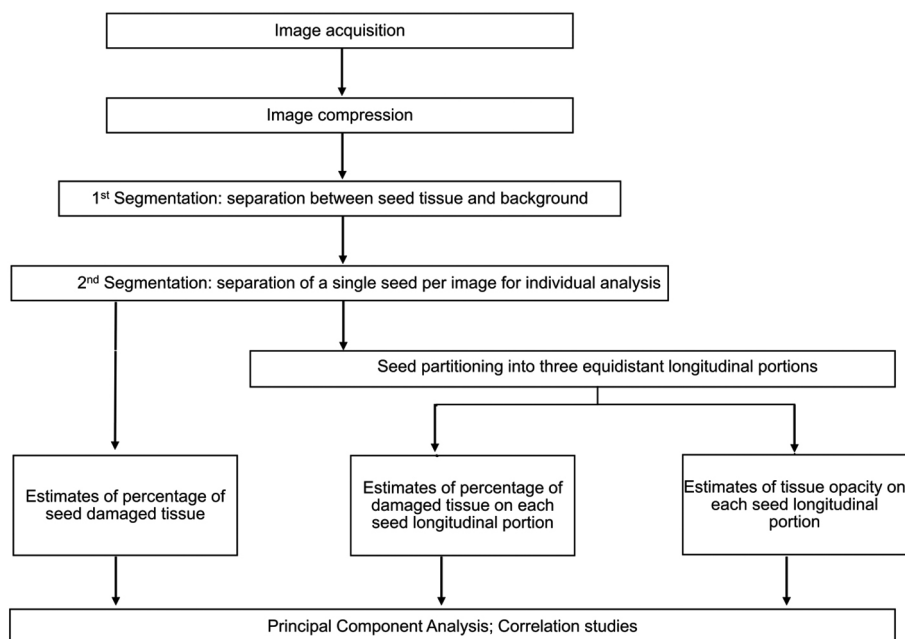


**Figure 1** – Fluxogram of procedures after image acquisition referring to segmentation and feature extraction.

damaged seed tissue (PercM1, PercM2, PercM3), opacity of damaged (OpacM1, OpacM2, OpacM3), and undamaged seed tissue (OpacV1, OpacV2, OpacV3). In addition, we also estimated the total damaged area of each seed (PercMt). Seed tissue opacity was given by the mean of the correspondent pixels, with pixel values varying from zero to one. The closer to zero, the lower the retention of X-ray waves and thus the lower the tissue opacity.

Pearson's correlation coefficients were estimated to verify the existence of a linear association between the variables obtained from imaging analysis and germination tests. Significant statistical correlations by the t-test at 0.05 significance level were represented graphically with the help of the *ggraph* package.

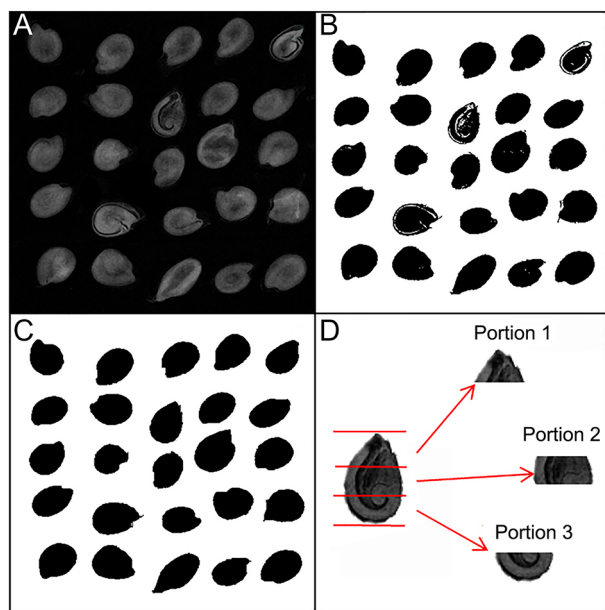


**Figure 2** – Steps of X-ray image processing of tomato seeds. Original image (A), Image segmented using a 0.10 threshold separating seed tissue from the background (B), filling in of seed dark or necrotic parts (C), and image partitioning in three equidistant longitudinal portions (D).

### Imaging analysis classification automation

The image of each seed was manually evaluated and graded according to the scale below (Figure 3).

Individual images were created for each seed, resulting in 4,600 images per growing season (25 seed images for each of the four replicates and the 46 accessions in each growing season). We then created a synthetic seed image dataset containing 2,000 images for training and 1,000 for validation. To do this, we created  $320 \times 320$  sized-images on a black background on which we overlapped the seed images. One to ten seed images were selected computationally in a random way. Seed position within the synthetic image, as well as seed rotation, were randomly established. The entire process was implemented using the *cocosynth* library (<https://github.com/akTwelve/cocosynth>).

The Mask R-CNN (He et al., 2017) was used ([https://github.com/matterport/Mask\\_RCNN](https://github.com/matterport/Mask_RCNN)) by the Keras library. The residual network ResNet101 (He et al., 2017) was used for the feature extraction. We performed fine-tuning using our synthetic seed image dataset from the initial weights of ResNet101 obtained by training using the MS COCO dataset. Configuration predefined by the repository, including the network architectures and losses, was used. Forty epochs were used by stochastic gradient descent optimization with a learning rate of 0.001 and batch size of two. Within the 3000 images of the synthetic dataset, 2000 were used for training and 1000 for validation. The synthetic training data have a fixed image size of  $320 \times 320$ ; however, the input image size for the network was not changed. A threshold value of 0.7 was defined to isolate the final mask regions.

After network training, the test was performed using X-ray images of seeds from the second growing season. To verify the Mask RCNN accuracy in detecting objects, we built a confusion matrix with the network's predicted classifications as a function of the manual classifications. We used the Recall, Accuracy, precision, and F-Measure metrics to assess network efficiency.

The material and methods used in this work are summarized in Figure 4.

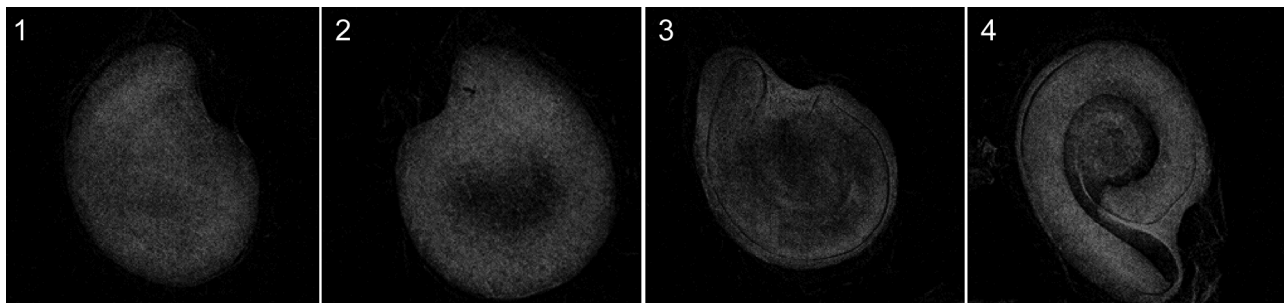


**Figure 3** – X-ray images of *Solanum lycopersicum* seeds manually classified into four categories. Undamaged (1), Partially undamaged (2), Partially damaged (3), Highly damaged (4).

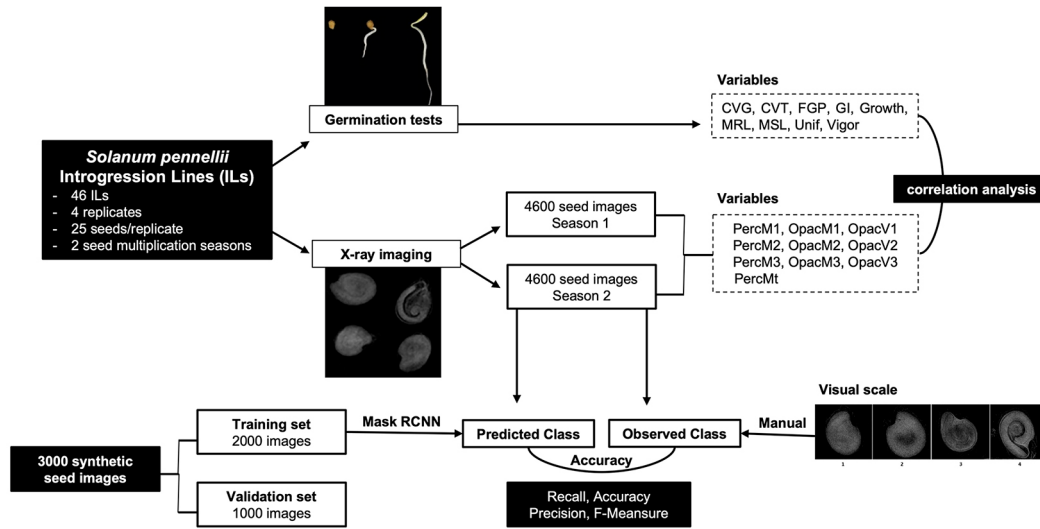


**Figure 4** – Flowchart summarizing the material and methods. PercMt = total damaged area of each seed; PercM1 = percentage of damaged seed tissue in portion 1; PercM2 = percentage of damaged seed tissue in portion 2; PercM3 = percentage of damaged seed tissue in portion 3; OpacM1 = opacity of damaged seed tissue on portion 1; OpacM2 = opacity of damaged seed tissue on portion 2; OpacM3 = opacity of damaged seed tissue on portion 3; OpacV1 = opacity of undamaged seed tissue on portion 1; OpacV2 = opacity of undamaged seed tissue on portion 2; OpacV3 = opacity of undamaged seed tissue on portion 3; FGP = final germination percentage; GI = germination index; CVT = coefficient of variation of germination time; CVG = coefficient of variation of germination; MSL = mean shoot length; MRL = mean root length; Unif = uniformity index, Growth = growth index; Vigor = vigor index.

## Results

### Treatment characterization

Treatment characterization regarding the tested variables is shown in Figure 5A-B. In this study, we observed variations in all the studied traits. Variables related to the percentage of damaged seed tissue and final germination showed both the lowest and highest estimates for both evaluation periods.

The accessions displayed different behavior depending on the evaluation period. The wild *S. pennellii* accession LA 716, for example, showed the highest estimates for CVT, Unif, and living tissue opacity-related variables in the first evaluation period. In contrast, the highest estimates were observed for FGP, GI CVT, MSL, and Unif in the second evaluation period. Genotypes with the greatest differences in performance between one evaluation period and the other being LA 3475, LA 4033, LA 4048, LA 4050, LA 4063, LA 4064, LA 4089, LA 4094, and LA 4098, where they displayed the lowest estimates for the Percm1 and Percm2 variables in the first period and the highest estimates in the second. The accession LA 4088 displayed high and low estimates for all Percm-related variables in the first and second evaluation periods, respectively. LA 4038 displayed high estimates for the OpacM-related variables in the first evaluation period and low estimates in the second. The LA 4098 accession differed the most between one evaluation period and the other when compared to

the other genotypes, with divergences found for the variables Percmt, Percm1, Percm2, Percm3, Opac2, Opac3, GS1, CVG, MSL, MRL, Growthtm, and Vigor.

On the other hand, specific genotypes displayed an analogous performance in both evaluation periods. The accessions LA 4046, LA 4043, and LA4047, for example, were considered to be uncommonly similar in both evaluation periods for all the tested variables. In addition, the Santa Clara commercial tomato cultivar showed low estimates for most of the variables tested in both evaluation periods.

### Association between descriptors obtained from the computational analysis of X-ray images of seeds and accession characterization

The graphical dispersion of Pearson's correlation estimates over image-based descriptors is presented in Figure 6. We observed a low correlation between the living tissue opacity group variables and the other variables. The highest values were in Opacv3 and Opacm2 ( $r = -0.51$ ). Positive high-magnitude correlations were found between variables within each group (Opacv, Opacm, and Percm), for example, the correlation between Opacv1 and Opacv3 ( $r = 0.87$ ), and between Opacv2 and Opacv3 ( $r = 0.84$ ) as well as the correlation between Opacm2 and Opacm3 ( $r = 0.86$ ). As for Percm, the correlation between Percm1 and Percm 2, and Percm1 and Percm 3 were equal to 0.95 and the correlation between Percm2 and Percm 3

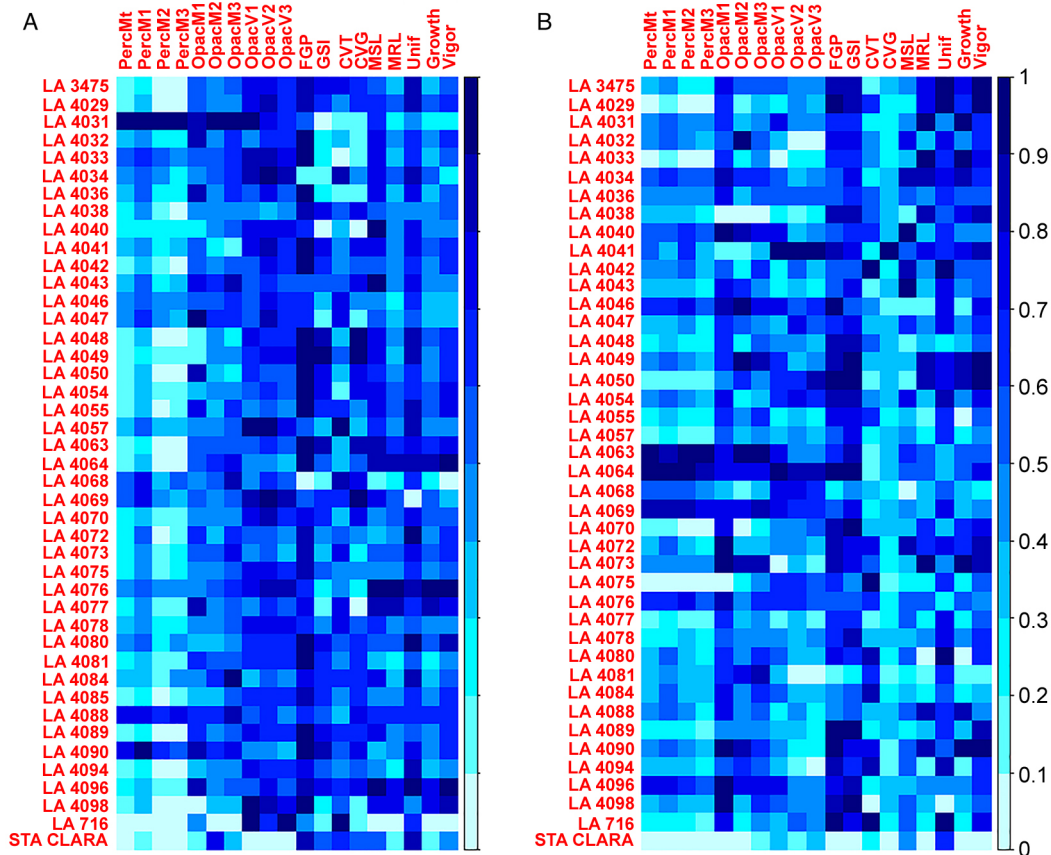


**Figure 5** – Representation of descriptors obtained from the computational analysis of X-ray images and the evaluation of seed and seedling's physiological traits of tomato accessions on the first (A) and second (B) evaluation periods. Variables' estimates were normalized to range from 0 to 1 for better graphical representation. PercMt = total damaged area of each seed; PercM1 = percentage of damaged seed tissue in portion 1; PercM2 = percentage of damaged seed tissue in portion 2; PercM3 = percentage of damaged seed tissue in portion 3; OpacM1 = opacity of damaged seed tissue on portion 1; OpacM2 = opacity of damaged seed tissue on portion 2; OpacM3 = opacity of damaged seed tissue on portion 3; OpacV1 = opacity of undamaged seed tissue on portion 1; OpacV2 = opacity of undamaged seed tissue on portion 2; OpacV3 = opacity of undamaged seed tissue on portion 3; FGP = final germination percentage; GI = germination index; CVT = coefficient of variation of germination time; CVG = coefficient of variation of germination; MSL = mean shoot length; MRL = mean root length; Unif = uniformity index; Growth = growth index; Vigor = vigor index.

to 0.97. Variables related to living tissue opacity showed low negative correlation with variables related to the percentage of damaged seed tissue, the highest value of correlation being between Opacv3 and Percm1 ( $r = -0.29$ ).

#### Association between descriptors obtained from computational analysis of X-ray images and parameters of physiological quality of seeds

Correlations were found between the physiological characteristics of seeds and the image-based characteristics, indicating that analyses of X-ray images could help predict the physiological quality of seeds (Figure 7A-I).

All physiological variables showed a significant correlation with the variable dead tissue opacity. Positive, high-magnitude correlations ( $r \geq 0.90$ ) were

observed for Unif and  $CVT \times OpcM3$ ; Unif and  $CVT \times OpacM2$ , and  $CVT \times OpacM1$ .

High negative correlation estimates ( $-0.70 \geq r \geq -0.90$ ) were observed for the variables OpcM1 with GI and Vigor; OpcM2 with FGP, GI, MSL, MRL, Growth, and Vigor; OpcM3 with GI, MSL, MRL, Growth, and Vigor; PercM1, 2, 3, and t with GI and Unif. Living tissue opacity was highly correlated ( $r = 0.83$ ) with CVG. These results indicate that seeds with low values for opacity and percentage of damaged seed tissue along with high values for living tissue opacity have greater physiological quality.

#### Seed classification through convolutional neural networks

Observed and predicted seed classification shown in Table 1. By observing the table's diagonal elements, the

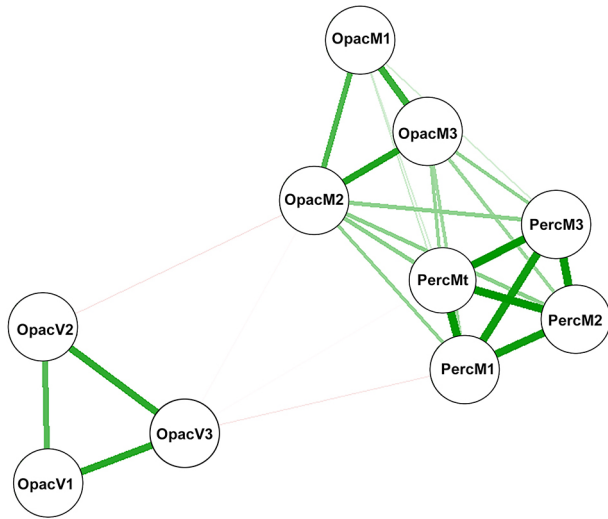


**Figure 6** – Graphical dispersion of Pearson's correlation estimates between descriptors obtained from computational analysis of X-ray images in tomato seeds. Green lines indicate positive correlations by the t-test ( $p \leq 0.05$ ). Line thickness is proportional to its magnitude. PercMt = total damaged area of each seed; PercM1 = percentage of damaged seed tissue in portion 1; PercM2 = percentage of damaged seed tissue in portion 2; PercM3 = percentage of damaged seed tissue in portion 3; OpacM1 = opacity of damaged seed tissue on portion 1; OpacM2 = opacity of damaged seed tissue on portion 2; OpacM3 = opacity of damaged seed tissue on portion 3; OpacV1 = opacity of undamaged seed tissue on portion 1; OpacV2 = opacity of undamaged seed tissue on portion 2; OpacV3 = opacity of undamaged seed tissue on portion 3.

majority of seeds could be correctly classified, with an overall accuracy of 83.64 %. In almost all cases, when a seed was misclassified, it was assigned to a neighboring class, probably due to the manual classification's subjectivity. Quick discrimination of seed physiological conditions by the human eye is challenging, supporting the need for more accurate approaches. The Kappa values were higher than 90 % for all classes, which, according to Landis and Koch (1977), indicates perfect agreement. The metrics precision, recall, and F-Measure were high for all classes. Class four showed the highest and class three the lowest values.

## Discussion

Seed quality is essential to the successful establishment and high yield of any crop. Therefore, the seed lots must be evaluated before marketing to determine their quality. Nowadays, seed quality is assessed mainly through germination and vigor tests followed by manual evaluation. Recent studies suggest that seed X-ray image analysis might be a valuable and efficient tool for assessing seed quality quickly and non-destructively in different crop species (Ahmed et al., 2018; Raju Ahmed

**Table 1** – Observed and predicted classes of seed physiological quality. Predicted classes were based on convolutional neural network analyses.

Observed Class	Predicted Class			
	1	2	3	4
1	297	67	3	0
2	127	1242	36	0
3	0	229	690	75
4	0	1	214	1619
Kappa (%)	95.69	96.05	93.08	91.78
Precision (%)	70.03	80.66	73.21	95.57
Recall (%)	80.92	88.39	69.40	88.28
F-Measure (%)	75.08	84.34	71.26	91.78
Overall Accuracy (%)	83.64			
Spearman's correlation	0.92			

et al., 2020). A bottleneck that poses a challenge to adopting this technology is processing the X-ray images to extract the data and then make inferences about seed quality. In light of this, the first valuable contribution of our work is the algorithm that we built. It uses computer vision to efficiently identify a seed in the X-ray image, segment it into three equally-sized portions, and infer about damage in the seed tissue of each portion through a grayscale matrix. The algorithm generated several variables to make inferences regarding seed quality. Therefore, it might be helpful for future studies using seed X-ray images.

According to the evaluated traits shown in Figure 5A-B, the genotype characterization highlights their genetic differences. In our study, except for the commercial cultivar Santa Clara, the only genetic difference between the genotypes is the small genomic segments of *S. pennellii* (LA716) replacing homologous regions in the M82 genome Eshed and Zamir (1995). We observed higher FGPvalues followed by lower values for damaged seed tissue in most genotypes. Damage to the seed's internal tissues usually leads to reductions in seed germination. Damage in the inner parts of the seed may have critical effects on its viability to germinate and develop power (Yu et al., 2018). This is most probably related to damage in the structure of the macromolecules structure and membranes' surface, which causes lower germination and vigor rates (Vasconcelos et al., 2018).

The different genotype behavior in the two growing seasons highlighted in Figure 5A-B reinforces the idea that environmental factors highly affect seed quality. Interaction between the maternal conditions where plants grew during seed production and the genotypic characteristics is determinant in defining the tomato seed quality (Geshnizjani et al., 2020). Seed quality may vary significantly from year to year and from one production site to another (Finch-Savage and Bassel, 2016). Therefore, slight differences in temperature, light, or soil humidity in the two growing seasons might have influenced seed formation and, consequently, seed quality.

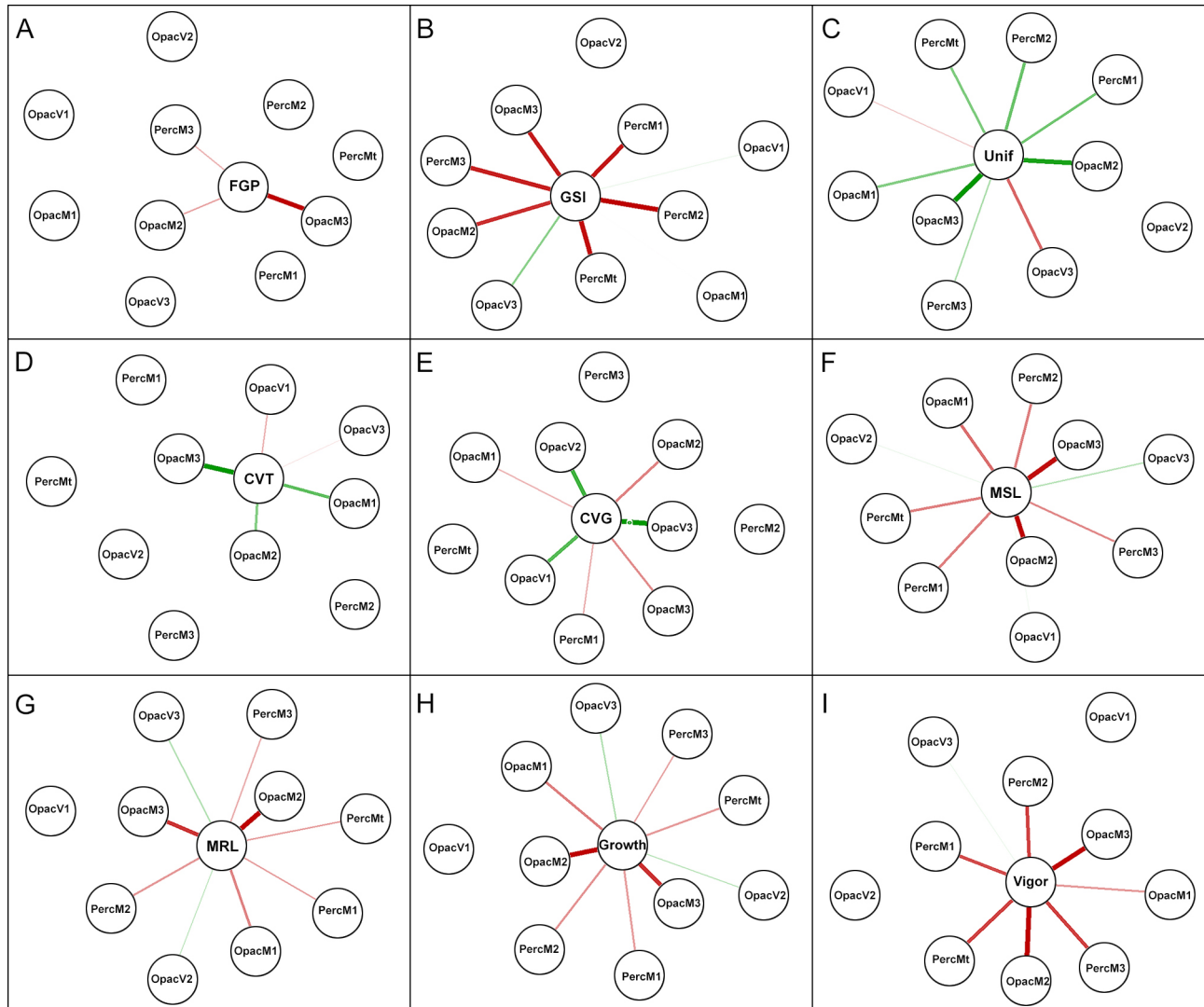


**Figure 7** – Graphical dispersion of Pearson's correlation estimates between physiological variables and variables obtained from computational analysis of X-ray images in tomato seeds (A-I). Green and red lines indicate positive and negative correlation, respectively, by the t-test ( $p \leq 0.05$ ). Line thickness is proportional to its magnitude. PercMt = total damaged area of each seed; PercM1 = percentage of damaged seed tissue in portion 1; PercM2 = percentage of damaged seed tissue in portion 2; PercM3 = percentage of damaged seed tissue in portion 3; OpacM1 = opacity of damaged seed tissue on portion 1; OpacM2 = opacity of damaged seed tissue on portion 2; OpacM3 = opacity of damaged seed tissue on portion 3; OpacV1 = opacity of undamaged seed tissue on portion 1; OpacV2 = opacity of undamaged seed tissue on portion 2; OpacV3 = opacity of undamaged seed tissue on portion 3; FGP = final germination percentage; GI = germination index; CVT = coefficient of variation of germination time; CVG = coefficient of variation of germination; MSL = mean shoot length; MRL = mean root length; Unif = uniformity index; Growth = growth index; Vigor = vigor index.

Although our results highlight the interaction between genotype  $\times$  growing season and the evaluated traits, the accessions LA 4046, LA 4043, and LA4047 presented similar results in both growing seasons. This result might indicate the stability of these genotypes pertaining to the evaluated traits. Phenotypic stability is defined as a genotype's ability to be least affected by environmental variations (Cruz et al., 2014). Genotypes with high stability for seed quality traits are crucial for the seed industry, especially for crops like tomatoes,

where the cost of a single seed is expressive. Therefore, these genotypes show promise as applications as genetic resources to these traits in future studies.

Correlation between traits measured through the specific algorithm constructed is displayed in Figure 6. Variables from the same group (OpacV, OpacM, and PercM) correlate more with one another than with variables from a different group. Furthermore, variables that make inferences about the damaged tissue are more correlated than those measuring the undamaged

tissue. The correlations between the physiological traits measured manually, and those image traits measured using computer vision through the specific algorithm constructed provide insights into how the X-ray image analysis can be useful whilst inferring seed quality. The seed's segmentation into three portions allowed us to dissect how damage in different parts of the seed can influence its overall germination and vigor. Portion one is related to the seed coat, whereas portions two and three are related to where the endosperm and cotyledon of tomato seeds are usually located (Downie et al., 1999). The segmentation is important since similar damages in different portions might impact on germination and seedling vigor differently. For example, light damage in the embryonic region might be more severe for this process than similar damage in the seed coat.

Seed morphology might be determinant in the development of healthy and uniform seedlings (Raju Ahmed et al., 2020). The seed morphology standard is related to the seed coat, endosperm or cotyledons, and embryo (Boesewinkel and Bouman, 1984). Each of them plays a different role during germination; the seed coat acts as a barrier protecting the inner parts and might contain chemicals that trigger dormancy under certain environmental conditions, while the cotyledons or endosperm are responsible for supplying nutrients to the embryo during germination (Meng et al., 2016).

Our study found that the opacity of the damaged tissue correlated with all the physiological traits evaluated. It was measured by considering the level of gray of the portion evaluated - the lighter the gray, the more expressive the tissue damage.

A positive high-magnitude correlation between OpacM and the physiological traits CVT and Unif was observed. The germination time variation is measured by CVT (Carvalho et al., 2005), whereas Unif measures the uniformity of the germination (Silva et al., 2019). As expected, the higher the OpacM value, the more severe the damage to the seed tissue; hence, the more significant variation in germination time. For Unif, as the seed tissue damage becomes more severe, the uniformity increases, which means that the seed lot's behavior is more homogeneous, though not necessarily better. Since we observed that the correlation between OpacM and FGP is negative and high-magnitude, indicating that the more severe the tissue damage, the lower the germination percentage, it can be postulated that the high Unif for seeds with high OpacM mostly indicates that they germinate uniformly although poorly.

The OpacM1 trait was highly negatively correlated with GI and Vigor. OpacM1 indicates the severity of the damage in the tissue of portion one, which is where the micropylar cap is located and is also the place where the radicle protrusion occurs. The GI trait measures the speed of the germination process (Silva et al., 2019), and Vigor considers the seedling growth, germination uniformity, and germination percentage (Medeiros and Pereira, 2018). Therefore, damage to this portion of the seed can lead to

delays in the radicle protrusion and negatively affect seed germination and vigor.

In this study, OpacM2 and OpacM3 were highly negatively correlated with most of the physiological traits. The seed portions 2 and 3 were related to the location of the cotyledons and the embryo. Therefore, it is expected that severe damage in these portions of the seed leads to reductions in its physiological quality. The germination speed coefficient, CVG, showed high positive correlation with OpacV in the three portions measured, meaning that the less the damage to the seed, the faster the germination occurs. In other words, from our data, we can infer that damage to the seed tissues leads to poor germination and vigor, which was also found in other studies using X-ray image analysis (Noronha et al., 2018; Medeiros et al., 2020a; Vasconcelos et al., 2018).

Our last findings refer to using CNN to classify tomato seed X-ray images. It is well known that optical technologies can detect changes that occurred in the seeds caused by different factors such as physiological disturbances during maturation, damage caused by improper storage conditions, tissue deterioration, or the action of insects and pathogens (Silva et al., 2018; Medeiros et al., 2020a). X-ray technology generates time and resource savings. It is simpler to execute and cheaper than more advanced techniques such as magnetic resonance imaging and multispectral imaging equipment, respectively. When the analysis of X-ray images is performed using human vision, the risks of error due to subjective interpretations and the time spent on the analysis increase significantly (Xia et al., 2019). Therefore, we propose herein the utilization of CNN as a valuable alternative to overcome these challenges.

Machine learning methods are often resorted to so as to interpret image analysis data. Among these methods, deep learning strategies such as convolutional neural networks (CNNs) are trends in artificial intelligence for this purpose. Studies with Mask region convolutional neural network (MaskRCNN) have demonstrated a strong capacity for recognizing targets (Machefer et al., 2020; Shi et al., 2019; Stewart et al., 2019). Typically, deep learning methods are used to analyze two-dimensional images. In this study, CNN showed promising results with an accuracy of 83.64 %. Moreover, the CNN mistakes in seed classification were usually due to assignments to a neighboring class; for example, a seed manually classified as one was CNN classified as two and vice versa, indicating the method's reliability.

F-measure can be simplistically interpreted as a metric that represents the harmonic mean of the two confusion matrix degrees of freedom: precision and recall (Hand et al., 2021). Recall is the proportion of real positive cases that are correctly predicted positive, and precision denotes the proportion of predicted positive cases that are correctly real positives (Powers, 2020). Recall indicates missed positive predictions, while precision only comments on the correct positive predictions out of all the positive predictions (Kynkäänniemi et al., 2019).

Combining these two metrics in one, the F-measure provides an individual score that balances the concerns of precision and recall. The high precision, recall, and F-measure values observed in this work, indicate the algorithm efficiency.

Convolutional neural network is being used in seed science for different purposes, such as identification of haploid and diploid seeds using images (Altuntaş et al., 2019), variety identification in rice and oats (Qiu et al., 2018; Wu et al., 2019), classification of hybrid seed using NIR (Nie et al., 2019), and oak acorn viability (Przybyło and Jabłoński, 2019). The use of CNN for the purpose described in this work is novel and proved to be an agile, non-destructive method that allows for rating seed viability and vigor with a high degree of accuracy.

The significant correlations between germination variables and image-based variables found in this study point to X-ray imaging analysis as representing a good tool for predicting seed quality on a large scale and in a non-destructive way. Yet, convolutional neural networks proved to be a reliable resource in the correct classification of seeds into quality classes, as only a few differences from the manual classification were found. The MaskRCNN approach still has the advantage of being less subjective than the manual approach and is therefore recommended.

## Acknowledgments

The authors are grateful to Agronomy and Entomology Departments (UFV – Universidade Federal de Viçosa, Viçosa, Brazil) for the experimental installations and Dr. Laércio Junio da Silva and M.Sc. André Dantas de Medeiros for the contribution in obtaining the images used in this work. This study was supported by the Coordenação de Aperfeiçoamento de Pessoal de Nível Superior (CAPES) (Finance Code 001), Fundação de Amparo à Pesquisa do Estado de Minas Gerais (FAPEMIG), and Conselho Nacional de Desenvolvimento Científico e Tecnológico (CNPq).

## Authors' Contributions

**Conceptualization:** Pessoa HP. **Formal analysis:** Azevedo AM. **Investigation:** Pessoa HP, Copati MGF, Dariva FD, Almeida GQ. **Methodology:** Pessoa HP. **Resources:** Gomes CN. **Software:** Azevedo, AM. **Supervision:** Gomes CN. **Validation:** Azevedo, AM. **Writing – original draft:** Pessoa HP, Copati MGF. **Writing – review & editing:** Copati MGF, Dariva FD, Almeida GQ, Azevedo AM, Gomes CN.

## References

Ahmed MR, Yasmin J, Collins W, Cho BK. 2018. X-ray CT image analysis for morphology of muskmelon seed in relation to germination. *Biosystems Engineering* 175: 183-193. <https://doi.org/10.1016/j.biosystemseng.2018.09.015>

- Altuntaş Y, Cömert Z, Kocamaz AF. 2019. Identification of haploid and diploid maize seeds using convolutional neural networks and a transfer learning approach. *Computers and Electronics in Agriculture* 163: 104874. <https://doi.org/10.1016/j.compag.2019.104874>
- Boesewinkel FD, Bouman F. 1984. The seed: structure. p. 567-610. In: Johri BM. ed. *Embryology of angiosperms*. Springer, Berlin, Germany.
- Carvalho MP, Santana DG, Ranal MA. 2005. *Anacardium humile* A. St.-Hil. (Anacardiaceae) seedling emergence evaluated by means of small samples. *Revista Brasileira de Botânica* 28: 627-633 (in Portuguese, with abstract in English). <https://doi.org/10.1590/S0100-84042005000300018>
- Cruz CD, Carneiro PCS, Regazzi AJ. 2014. *Biometric Models Applied to Genetic Improvement = Modelos Biométricos Aplicados ao Melhoramento Genético*. 3ed. Editora UFV, Viçosa, MG, Brazil (in Portuguese).
- Downie B, Gurusinghe S, Bradford KJ. 1999. Internal anatomy of individual tomato seeds: Relationship to abscisic acid and germination physiology. *Seed Science Research* 9: 117-128. <https://doi.org/10.1017/S0960258599000136>
- Eshed Y, Zamir D. 1995. An introgression line population of *Lycopersicon pennellii* in the cultivated tomato enables the identification and fine mapping of yield-associated QTL. *Genetics* 141: 1147-1162. <https://doi.org/10.1093/genetics/141.3.1147>
- Finch-Savage WE, Bassel GW. 2016. Seed vigour and crop establishment: extending performance beyond adaptation. *Journal of Experimental Botany* 67: 567-591. <https://doi.org/10.1093/jxb/erv490>
- Geshnizjani N, Snoek BL, Willems LAJ, Rienstra JA, Nijveen H, Hilhorst HWM, et al. 2020. Detection of QTLs for genotype × environment interactions in tomato seeds and seedlings. *Plant Cell and Environment* 43: 1973-1988. <https://doi.org/10.1111/pce.13788>
- Hand DJ, Christen P, Kirielle N. 2021. F\*: an interpretable transformation of the F-measure. *Machine Learning* 110: 451-456. <https://doi.org/10.1007/s10994-021-05964-1>
- He K, Gkioxari G, Dollár P, Girshick R. 2017. Mask R-CNN. *Proceedings of the IEEE. IEEE Computer Society, Venice, Italy*. <https://doi.org/10.1109/ICCV.2017.322>
- Jin X, Jie L, Wang S, Qi HJ, Li SW. 2018. Classifying wheat hyperspectral pixels of healthy heads and *Fusarium* head blight disease using a deep neural network in the wild field. *Remote Sensing* 10: 395. <https://doi.org/10.3390/rs10030395>
- Kotwaliwale N, Singh K, Kalne A, Jha SN, Seth N, Kar A. 2014. X-ray imaging methods for internal quality evaluation of agricultural produce. *Journal of Food Science and Technology* 51: 1-15. <https://doi.org/10.1007/s13197-011-0485-y>
- Kynkäänniemi T, Karras T, Laine S, Lehtinen J, Aila T. 2019. Improved precision and recall metric for assessing generative models. *Advances in Neural Information Processing Systems* 32: 1-16. <https://doi.org/10.48550/arXiv.1904.06991>
- LeCun Y, Bengio Y, Hinton G. 2015. Deep learning. *Nature* 521: 436-444. <https://doi.org/10.1038/nature14539>
- Machefer M, Lemarchand F, Bonnefond V, Hitchins A, Sidiropoulos P. 2020. Mask R-CNN refitting strategy for plant counting and sizing in UAV imagery. *Remote Sensing* 12: 3015. <https://doi.org/10.3390/rs12183015>

- Medeiros AD, Pereira MD. 2018. SAPL®: a free software for determining the physiological potential in soybean seeds. *Pesquisa Agropecuária Tropical* 48: 222-228. <https://doi.org/10.1590/1983-40632018v48i2340>
- Medeiros AD, Pinheiro DT, Xavier WA, Silva LJ, Dias DCFS. 2020a. Quality classification of *Jatropha curcas* seeds using radiographic images and machine learning. *Industrial Crops and Products* 146: 112162. <https://doi.org/10.1016/j.indcrop.2020.112162>
- Medeiros AD, Silva LJ, Pereira MD, Oliveira AMS, Dias DCFS. 2020b. High-throughput phenotyping of brachiaria grass seeds using free access tool for analyzing X-ray images. *Anais da Academia Brasileira de Ciências* 92: 1-16. <https://doi.org/10.1590/0001-3765202020190209>
- Meng LS, Wang YB, Loake GJ, Jiang JH. 2016. Seed embryo development is regulated via an *AN3-MIN13* gene cascade. *Frontiers in Plant Science* 7: 1645. <https://doi.org/10.3389/fpls.2016.01645>
- Nie P, Zhang J, Feng X, Yu C, He Y. 2019. Classification of hybrid seeds using near-infrared hyperspectral imaging technology combined with deep learning. *Sensors and Actuators B: Chemical* 296: 126630. <https://doi.org/10.1016/j.snb.2019.126630>
- Noronha BG, Medeiros AD, Pereira MD. 2018. Assessment of the physiological quality of *Moringa oleifera* Lam. seeds. *Ciência Florestal* 28: 393-402 (in Portuguese, with abstract in English). <https://doi.org/10.5902/1980509831615>
- Pang L, Men S, Yan L, Xiao J. 2020. Rapid vitality estimation and prediction of corn seeds based on spectra and images using deep learning and hyperspectral imaging techniques. *IEEE Access* 8: 123026-123036. <https://doi.org/10.1109/ACCESS.2020.3006495>
- Pinto MS, Damasceno Junior PC, Oliveira LC, Machado AFF, Souza MAA, Muniz DR, et al. 2018. Diversity between *Jatropha curcas* L. accessions based on oil traits and X-ray digital images analysis from it seeds. *Crop Breeding and Applied Biotechnology* 18: 292-300. <https://doi.org/10.1590/1984-70332018v18n3a43>
- Powers DMW. 2020. Evaluation: from precision, recall and F-measure to ROC, informedness, markedness and correlation. <https://doi.org/10.48550/arXiv.2010.16061>
- Przybyło J, Jabłoński M. 2019. Using deep convolutional neural network for oak acorn viability recognition based on color images of their sections. *Computers and Electronics in Agriculture* 156: 490-499. <https://doi.org/10.1016/j.compag.2018.12.001>
- Qiu Z, Chen J, Zhao Y, Zhu S, He Y, Zhang C. 2018. Variety identification of single rice seed using hyperspectral imaging combined with convolutional neural network. *Applied Sciences* 8: 212. <https://doi.org/10.3390/app8020212>
- Raju Ahmed M, Yasmin J, Wakholi C, Mukasa P, Cho BK. 2020. Classification of pepper seed quality based on internal structure using X-ray CT imaging. *Computers and Electronics in Agriculture* 179: 105839. <https://doi.org/10.1016/j.compag.2020.105839>
- Rippner DA, Raja PV, Earles JM, Momayyezi M, Buchko A, Duong FV, et al. 2022. A workflow for segmenting soil and plant X-ray computed tomography images with deep learning in Google's Colaboratory. *Frontiers in Plant Science* 13. <https://doi.org/10.3389/FPLS.2022.893140>
- Sahin ME. 2023. Image processing and machine learning-based bone fracture detection and classification using X-ray images. *International Journal of Imaging Systems and Technology*. <https://doi.org/10.1002/IMA.22849>
- Shi W, van de Zedde R, Jiang H, Kootstra G. 2019. Plant-part segmentation using deep learning and multi-view vision. *Biosystems Engineering* 187: 81-95. <https://doi.org/10.1016/j.biosystemseng.2019.08.014>
- Silva LJ, Dias DCFS, Sekita MC, Finger FL. 2018. Lipid peroxidation and antioxidant enzymes of de *Jatropha curcas* L. seeds stored at different maturity stages. *Acta Scientiarum. Agronomy* 40: 1-10. <https://doi.org/10.4025/actasciagr.2018.v40i1.34978>
- Silva LJ, Medeiros AD, Oliveira AMS. 2019. SeedCalc, a new automated R software tool for germination and seedling length data processing. *Journal of Seed Science* 41: 250-257. <https://doi.org/10.1590/2317-1545v42n2217267>
- Stewart EL, Wiesner-Hanks T, Kaczmar N, DeChant C, Wu H, Lipson H, et al. 2019. Quantitative phenotyping of northern leaf blight in UAV images using deep learning. *Remote Sensing* 11: 2209. <https://doi.org/10.3390/rs11192209>
- Tajbakhsh N, Shin JY, Gurudu SR, Hurst RT, Kendall CB, Gotway MB, et al. 2016. Convolutional neural networks for medical image analysis: full training or fine tuning? *IEEE Transactions on Medical Imaging* 35: 1299-1312. <https://doi.org/10.1109/tmi.2016.2535302>
- Vasconcelos MC, Costa JC, Silva-Mann R, Oliveira AS, Bárbara CNV, Carvalho MLM. 2018. Image analysis and health of *Moringa oleifera* seeds. *Comunicata Scientiae* 9: 590-595. <https://doi.org/10.14295/cs.v9i4.2980>
- Wu N, Zhang Y, Na R, Mi C, Zhu S, He Y, et al. 2019. Variety identification of oat seeds using hyperspectral imaging: investigating the representation ability of deep convolutional neural network. *RSC Advances* 9: 12635-12644. <https://doi.org/10.1039/C8RA10335F>
- Xia Y, Xu Y, Li J, Zhang C, Fan S. 2019. Recent advances in emerging techniques for non-destructive detection of seed viability: a review. *Artificial Intelligence in Agriculture* 1: 35-47. <https://doi.org/10.1016/j.aiaa.2019.05.001>
- Yu X, Lu H, Liu Q. 2018. Deep-learning-based regression model and hyperspectral imaging for rapid detection of nitrogen concentration in oilseed rape (*Brassica napus* L.) leaf. *Chemometrics and Intelligent Laboratory Systems* 172: 188-193. <https://doi.org/10.1016/j.chemolab.2017.12.010>